Further details can be found in:

M. Righi, G. Tardioli, L. Cascio, W. J. R. Hoefer, “Time Domain Characterization of Packaging Effects via Segmentation Technique“ to be published on the Special Issue on Packaging Effects and Interconnects of the MTT-S IEEE Transactions, September 1997.

4) Modal Boundary Conditions for Waveguides of Arbitrary Cross-section with SCN TLM

(Jonathan Herring, Mario Righi, Wolfgang J. R. Hoefer)

Modal absorbing boundary conditions have been applied to a graded mesh using the hybrid node, and to homogeneous waveguides of arbitrary cross-section. The best performance is obtained with rectangular waveguides but examples show that the method can also be used for other geometries. A T-junction circular-to-sidecoupled rectangular waveguide example is given.

For rectangular waveguides, the modal field distribution is well known. In the application of modal boundary conditions to TLM, it is convenient to work directly with the voltage pulses, rather than with the total tangential field components. This is possible because the link-line voltages are a linear combination of the electric and magnetic fields. For a graded mesh using the hybrid node, three different impedances are assigned to the three sets of link-lines contributing to each component of the magnetic field. The modal Green’s function is determined by the timestep and the node dimension perpendicular to the boundary; it is independent of the mesh grading in the cross-section.

Typical Green’s functions for the dominant mode in a WR28 waveguide are shown in the frequency domain in fig. 1, for the cases of (*i*) cubic nodes with the maximum timestep, (*ii*) cubic nodes with half the maximum timestep, and (*iii*) cuboid nodes of twice the length in the perpendicular direction and with the maximum timestep.

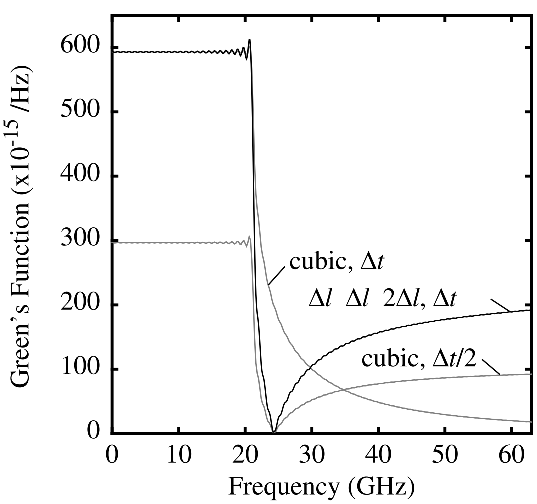

Fig. 1 – Modal Green’s functions for hybrid node

As the frequency increases, the curves tend towards the link-line reflection coefficient needed to match the TLM mesh to free-space:

$$\rho_l = \frac{\Delta l_{min} - \Delta l}{\Delta l_{min} + \Delta l} \qquad \text{where} \qquad \frac{l_{imn}}{t} = 2c\ \Delta t$$

Δl is the perpendicular node spacing, Δt is the timestep and c is the speed of light.

For homogeneous waveguides of arbitrary cross-section, the mode configuration can be obtained from two previous two-dimensional simulations. It is convenient to use a slice of three-dimensional nodes for this purpose. The cutoff frequencies are obtained from the first simulation and then, in the second, the Fourier transform of the appropriate voltage pulses is computed at these frequencies over the whole plane.

To form the modal coupling matrix, the complex output from the Fourier transform must be converted to real numbers. The magnitude can be taken if the field is orientated in a single direction. The resulting matrix can be used directly to convert from mode amplitudes to TLM voltage pulses. To convert back to mode amplitudes, a new matrix is formed in which each element is multiplied by the area of the corresponding node, and then a scaling factor is applied so that the conversions *to modes* and *from modes* are consistent. The voltage pulses incident on the boundary are then multiplied by the elements of this matrix.

The reflection coefficient of practical ABC's can be calculated as an S-parameter, from a knowledge of the total voltage and the incident voltage at the input port. The reference structure is used to obtain the incident voltage, and the length is chosen so that voltage pulses reflected from the ends of the waveguide are not visible at the output point, within the duration of the simulation.

Typical results are shown in fig. 2 for a ridged waveguide modelled at two different resolutions (32 by 16 nodes and 64 by 32 nodes) and for a circular waveguide.

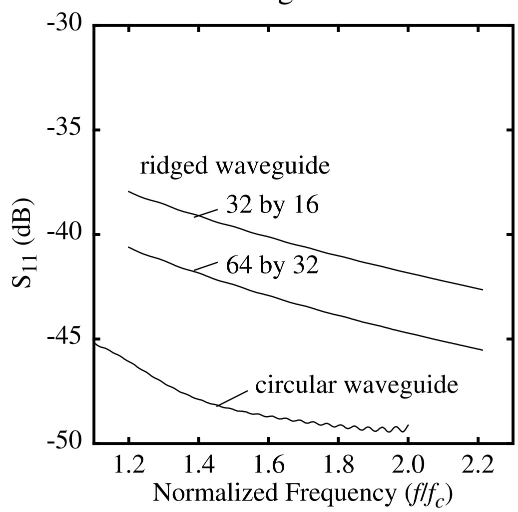

Fig 2 – Spurious reflection coefficient for ridged and circular waveguides terminated with modal ABC's

For rectangular waveguides, the performance of modal ABC's approaches the limit of numerical precision. Spurious reflections as low as -120dB are obtained with single precision arithmetic and -300dB with double precision.

The ABC's for uniform waveguides of arbitrary shape have been applied to the circular ports of the circular-to-rectangular T-junction shown in fig. 3a. A standard modal ABC for rectangular waveguides was used on port 3. Only the dominant modes were considered. The ABC's were therefore placed away from the junction, to ensure that all higher order modes would be sufficiently decayed. The entire structure was discretized on a cubic mesh with 28 cells in the diameter of the circular waveguide. The S-parameters are shown in fig. 3b, along with results obtained with a mode matching approach. Similar TLM results can be obtained with one-way equation ABC's, although there is always the potential for instabilities with this type of boundary.

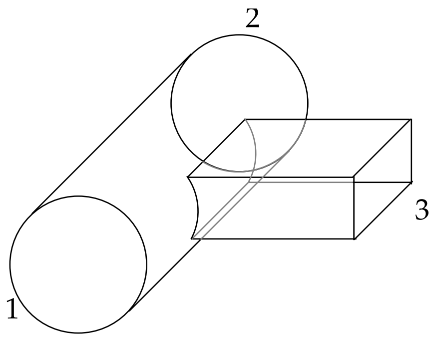

Fig.3a – Geometry of the circular to sidecoupled rectangular waveguide T-junction. Radius: 7.0 mm, rectangular waveguide: WR-62 (16.0 mm by 8.0 mm)

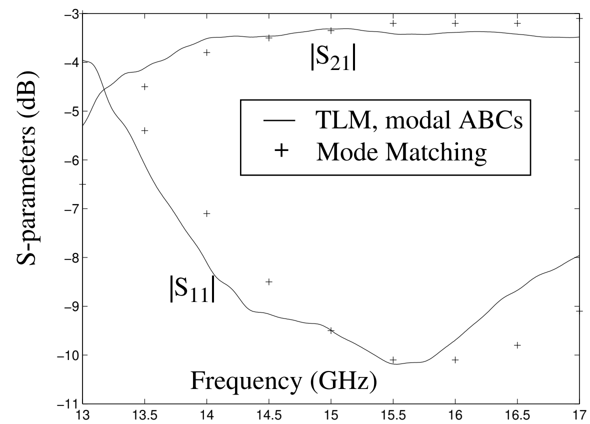

Fig.3b – Magnitude of the S-parameters of the circular to sidecoupled rectangular waveguide T-junction.

Further details can be found in:

J. L. Herring, M. Righi, W.J.R. Hoefer, "Modal Boundary Conditions For Waveguides of Arbitrary Cross-section With SCN TLM" in 1997 Intl. Microwave Symposium Dig., pp. 325-328, Denver, Colorado, June 9-13, 1997.

5) RF drying of softwood lumber in collaboration with the Faculty of Wood Science in UBC

(Mario Righi, Jonathan Herring, Wolfgang J. R. Hoefer and UBC team)

In the course of this research project a time domain model for the RF drying of wood in a vacuum kiln has been developed. The model includes the following physical phenomena involved in the drying of wood:

- Electromagnetic field distribution in the wood and the surrounding kiln,
- Energy deposition which increases the mobility of moisture in the lumber,
- Heat transfer and
- Mass transfer which, in turn, changes the dielectric properties of the wood.

The project aims at coupling all these phenomena in a self-consistent numerical model in space and time. Validation of the simulated results will be performed using the experimental RF/Vacuum Kiln available at UBC.

In order to cast the numerical models into a form directly amenable to experimental verification, the algorithms were implemented for a geometry resembling that of the UBC experimental kiln which is